Sustainable Food Technology

ROYAL SOCIETY OF CHEMISTRY

PAPER

View Article Online
View Journal | View Issue

Cite this: *Sustainable Food Technol.*, 2025, **3**, 1793

Microwave vacuum drying of Concord grape (*Vitis labrusca*) pomace: drying kinetics and quality attributes for enhanced valorization

Viral Shukla, Olga I. Padilla-Zakour and Chang Chen *

Concord grape (*Vitis labrusca*) pomace is a major processing waste and a valuable byproduct from the grape food industry that needs to be valorized. Microwave vacuum drying (MVD) was studied as a novel efficient technology to dry Concord grape pomace. Pomace cubes were dried under 8 kPa vacuum at 540, 1080, 2160 W microwave powers. Hot air drying (HAD) at 60 °C was used for comparison. The drying time, drying rates, effective moisture diffusivity, color metrics, and phenolic contents were experimentally determined. Drying kinetics during MVD were studied using the Page model and a mechanistic model coupling heat and moisture transfer characteristics. MVD reduced pomace moisture from 79% to 5% wet basis in 20–50 min, with 10-times higher average drying rates than HAD. The effective moisture diffusivity during MVD ranged from 1.1×10^{-7} to 3.4×10^{-7} m^2 s^{-1}, which increased with the increase in power density (W g^{-1}) and decrease in sample moisture. The mechanistic and empirical models fitted the validation data well (R_{adj}^2 = 0.970 to 0.998). The pomace color was preserved without significant influences (p > 0.05) by drying time nor microwave power. The total polyphenolic content increased with the decrease in sample moisture, but not significantly influenced by the microwave power. Findings from this study suggest that MVD is a promising drying method for the grape industry to valorize grape pomace with improved quality and sustainability.

Received 8th May 2025
Accepted 20th August 2025

DOI: 10.1039/d5fb00189g

rsc.li/susfoodtech

Sustainability spotlight

We believe that the results reported in this manuscript align well with the SDG 2 "End Hunger", specifically related goal "Food Security, and Nutrition and Sustainable Agriculture. This work provides a basis for clean methods for drying upcycled food products. We believe this work helps lead to ending hunger by reducing food loss and creating new value-added upcycled food and ingredients. We also believe the findings will be helpful for the grape industry to upcycle the pomace into value-added products.

1 Introduction

Concord (*Vitis labrusca*) is a common grape cultivar primarily used to produce juice with approximately 420 000 tons of annual production in the US.[1] The juicing process creates a significant amount of pomace byproduct (~25% by harvest weight) comprising of grape skin (~42%), seeds (~22%), and stems (~25%) with 50–72% moisture content, at an estimated 5 tons per hectare of vineyard.[2,3] Although grape pomace contains valuable bioactive compounds (polyphenols, anthocyanins, dietary fibers) with health benefits,[4,5] it has conventionally been discarded, which leads to food waste and negative impacts on waterways and land due to its high chemical oxygen demand.[6] Valorization of this valuable bioresource by developing value-added products could improve the grower's profitability, promote production and mitigate its environmental impact for better sustainability. The US, European Union and food companies are issuing bans or restrictions on many artificial food colors, including Red No. 3, Citrus Red 2, Orange B, and Red 40. Grape pomace's valorization can lead to the development of clean label ingredients. Pomace is a source of red anthocyanins which lends to upcycling opportunities as a natural colorant to replace artificial ones. Additionally, its high fiber and low sugar content lends its use as an added fiber source. Valorizing the Concord grape pomace could represent 105 000-ton waste reduction and recovering the bioactive compounds as valuable natural food ingredients, which would add economic benefits to grape growers and processors. However, due to the high moisture content, fresh grape pomace has a short shelf life. This emphasizes the need for developing efficient drying methods to preserve these nutrients and extend the shelf-life of grape pomace as a food ingredient.

The drying of bioproducts is an intensive and dynamic process that involves heat and mass transfer, as well as complex physical and chemical changes.[7] Conventionally, natural drying

Cornell AgriTech, Department of Food Science, Cornell University, Geneva, NY 14856, USA. E-mail: cc2774@cornell.edu; Tel: +1-315-787-2259

(sun drying) and hot air (HA) drying have been widely used for foods and agricultural products.[8] However, the natural or forced convective heat and mass transfer mechanisms usually result in low drying rates and efficiency, loss of product due to delayed drying, non-uniform drying and inconsistent product quality.[9,10] Various drying technologies have been used for the dehydration of grape pomace, which include sun drying,[11] HA drying;[12] vacuum drying;[13] infrared drying and freeze drying.[14] Although many of these methods are more efficient than the conventional practices, it was noted that the bioactive compounds in grape pomace are heat sensitive and could degrade rapidly under moderate to high temperature conditions.[15] Therefore, developing more suitable drying methods is critical in the processing of high-quality grape pomace and products in a cost- and time-efficient manner.

In recent years, developing sequential or combined drying technologies draws increasing interests in the food processing research. Among them, microwave vacuum drying (MVD) is a promising drying technology. MVD synergizes the advantages of microwave (MW) heating and vacuum, and selectively enhances the heat and mass transfer during the drying process. Under the vacuum conditions, water can evaporate at much lower temperatures, which significantly reduces the resistance to mass transfer during the drying process.[16] Compared to the conventional drying methods, during which thermal energy is received by the food surface by convection and transport inwards through conduction, MW penetrates the foods and 'activate' the polar substances (including ions and water molecules), leading to dipole vibrations and internal heat generation.[17] This 'volumetric heating' effect significantly overcomes the limitation of regular vacuum drying process due to the absence of air movement and convective heat transfer. In addition, the relatively low temperature and oxygen conditions under the MVD protect the heat labile bioactive constituents such as anthocyanins from degradation and oxidation.[15] MVD has been used for various foods, such as cranberries,[18] dried honey[19] and dried milk[20] but has not been reported in the valorization of grape pomaces.

Drying kinetics provides important information for understanding the change of drying rates and other product qualities and determining the most suitable processing conditions for food processors. Study of drying kinetics relies on both experimentation and mathematical modeling approaches, which can be further classified into empirical and mechanistic models.[21] The empirical models rely on the curve fitting of drying curves using regression equations. Dumpler & Moraru[20] used the Page model to study the drying kinetics of skim milk under a pilot scale MVD process. The mechanistic modeling approaches are based on fundamental mass transfer laws. Determination of effective moisture diffusivity is critical in the mechanistic modeling of the drying process. Several studies have been performed to determine the moisture diffusion characteristics during many MW-involved drying process, such as pomegranate arils,[22] grape seed,[23] and okra.[24]

The aim of this research was to study the drying kinetics of grape pomace under MVD using experimental and modeling approaches, and to quantitatively understand the quality change kinetics of it during the drying process for enhanced valorization of this future food ingredient.

2 Materials and methods

2.1 Processing

2.1.1 Pomace preparation. Concord (*Vitis labrusca* L.) pomace (skin, pericarp, seeds) was obtained from a juice manufacturing factory in upstate New York. Pomace was stored in 55-gallon drums and frozen at −20 °C immediately after juice pressing until use. The frozen pomace was fully defrosted in a 4 °C cold room before homogenization. Defrosted pomace was ground into a uniform paste using a Microcut (Stephan Microcut MC15, Riga, Latvia) with the addition of deionized water as necessary to obtain a uniform puree and initial moisture content of 79% on wet basis. The resulting paste was rapidly cooled, then frozen in aliquots until use.

2.1.2 Drying experiment. Drying experiments were performed in a pilot scale MVD dryer and a pilot scale HA dryer. For MVD, 30 g of pomace was loaded into the 3 cm × 3 cm cube cells of titanium silicone ice-cube trays (3 cells per tray, 4 trays, 360 g in total). Pomace was placed into non-adjacent cells to minimize the heat transfer across cells. The four trays were placed equidistant in the dryer to ensure even processing. Samples and trays were defrosted at 4 °C before drying to ensure the uniformity of starting shape and temperature.

During MVD, samples were treated at a total power of 540, 1080, 2160 W (initial power density of 1.5, 3, 6 W g^{-1}) and 8 kPa pressure using a commercial/pilot scale MVD dryer that is equipped with ten, 1000 W magnetrons at 2.45 GHz (Enwave, Delta, British Columbia, Canada). Samples were loaded to a Teflon rotary carrousel inside the drying oven, which was set to a ∼8 rpm speed to improve drying uniformity. Pomace were dried until no further absorption of microwaves could be sustained at that power level, which was corroborated by the onboard sensor indicating a drop in microwave absorption. Sample temperature was measured using an infrared radiometer that was equipped on the equipment. After drying, samples were removed from the chamber and weighed immediately, then sealed in freezer Ziploc bags and frozen until further analysis.

For HA drying, 30 g pomace cubes were loaded onto stainless steel trays (90 g per tray) and dried at 60 °C and 5% relative humidity (RH) in a HA dryer (Nyle Systems, Brewer, Maine, USA) with duplicates to mimic typical drying parameters.[25] The drying chamber temperature was digitally controlled, and the fluctuations were within ±1 °C and ±2% RH. Samples were dried until no significant difference in weight from previous time point.

2.2 Physicochemical characteristics

2.2.1 Color metrics. Color metrics of the grape pomace were determined by a portable colorimeter under the Hunter Lab's L*-a*-b* coordinates (Konika Minolta, Tokyo, Japan) using illuminant D65 and 10° observer angle. Six repeated

measurements were taken from the exposed surface of each sample.

2.2.2 Polyphenolic content. Total polyphenol content (TPC) was determined using the Folin-Ciocalteu method.[26] Pomace was extracted using absolute methanol under dark and constant agitation for 1 h. The amount of pomace extracted was based on the dry matter to account for change in water content and concentration of solids. The extracts were reacted with Folin–Ciocalteu reagent and incubated at room temperature. The reaction was then quenched with sodium carbonate solution then measured for absorbance at 765 nm using a UV-visible spectrophotometer (Thermo Fisher; Waltham, MA, USA). TPC was calculated as total available gallic acid equivalents (mg GAE/g dry pomace). The change of TPC was fitted to a 2nd order polynomial equation with sample moisture:

$$\mathrm{TPC} = A\ \mathrm{MC}^2 + B\ \mathrm{MC} + C \tag{1}$$

where MC is the moisture content of the pomace (kg water/kg wet mass); A, B, and C are regression coefficients.

2.3 Drying analysis

2.3.1 Drying kinetics. The moisture content of the grape pomace was determined using a gravimetric method. Specifically, the samples were dried in analytical duplicates of each triplicate in a conventional oven (Thermo Fischer, Waltham, MA, USA) at 105 °C for 24 h or until no change in mass between two adjacent measurements.[27] The moisture content on dry basis (M_{DB}) was calculated using eqn (2).

$$M_{\mathrm{DB}} = \frac{m_t - m_{\mathrm{d}}}{m_{\mathrm{d}}} \tag{2}$$

where m_t and m_{d} are the instantaneous mass at drying time t and dry mass (g) of the sample, respectively.

Moisture ratio (MR) was calculated from eqn (3):

$$\mathrm{MR} = \frac{M_t - M_{\mathrm{e}}}{M_0 - M_{\mathrm{e}}} \tag{3}$$

where M_t, M_0, M_{e} are the moisture content after drying at time t, before drying, and at equilibrium. M_{e} was set to 0.034 kg water/kg wet mass, which was determined experimentally.

Drying rate (DR) between two discrete time points was calculated from eqn (4).

$$\mathrm{DR} = \frac{\mathrm{MR}_{t-1} - \mathrm{MR}_t}{t_t - t_{t-1}} \tag{4}$$

The Page model was used to fit the drying data (eqn (5)). The Page model was selected due to its simplicity and reasonable accuracy in fitting most food drying data. This would minimize the overfitting concern that is common to empirical models with more regression coefficients.

$$\mathrm{MR} = e^{-k \times t^n} \tag{5}$$

where k, and n are the slope and shape parameter respectively.

2.3.2 Effective moisture diffusivity. The effective moisture diffusivity (D_{eff}) during the MVD process was calculated based on Fick's law of diffusion. The following assumptions were made for simplicity and reasonable accuracy.[28]

1. Moisture was evenly distributed within the pomace cubes;
2. The initial chemical compositions and physical properties of the pomace were homogenous and isotropic;
3. Effective moisture diffusivity was constant only within the short time intervals between the two adjacent sampling time points (≤5 min);
4. Shape changes of the pomace cubes were not significant during the drying process.

The general Fick's diffusion equation in two dimensional is written in the following form:

$$\frac{\partial \mathrm{MR}}{\partial t} = D_{\mathrm{eff}}\left(\frac{\partial^2 \mathrm{MR}}{\partial x^2} + \frac{\partial^2 \mathrm{MR}}{\partial y^2}\right) \tag{6}$$

where, D_{eff} is the effective moisture diffusivity ($\mathrm{m^2\ s^{-1}}$).

The D_{eff} values were determined from the analytical solution of Fick's diffusion equation in an infinite series format for a slab geometry with slight modification:[29]

$$\mathrm{MR} = 1 - \frac{8}{\pi^2}\sum_{n=0}^{\infty}\frac{\exp\left(-\dfrac{D_{\mathrm{eff}}(2n+1)^2\pi^2 t}{l^2}\right)}{(2n-1)^2} \tag{7}$$

where t is the drying time (s); l is the characteristic length of the sample (m), which is taken as the length of the cube in this study.

Eqn (7) can be further simplified by truncating to the first term (eqn (8)) when the falling-rate drying stage dominates the drying processes.

$$\mathrm{MR} = \frac{8}{\pi^2}\exp\left(-\frac{D_{\mathrm{eff}}\pi^2 t}{l^2}\right) \tag{8}$$

The average effective moisture diffusivity (D_{avg}, $\mathrm{m^2\ s^{-1}}$) during the drying process under each MW power levels was calculated as an arithmetic average of time-wise diffusivity values at different MC:[30,31]

$$D_{\mathrm{avg}} = \left(\sum_{1}^{n}\frac{D_{\mathrm{eff}}}{n}\right) \tag{9}$$

The mathematical correlation between the effective moisture diffusivity and sample moisture and MW power were developed using regression modeling approaches. Specifically, the moisture effect was modeled using polynomial equations (eqn (10)).

$$D_{\mathrm{eff}} = A\cdot\mathrm{MC}^3 + B\cdot\mathrm{MC}^2 + C\cdot\mathrm{MC} + D \tag{10}$$

where, A, B, C and D are the regression coefficients.

Uncertainty values of the effective moisture diffusivity attributed to the experimental and computation errors were evaluated using a method described by Holman.[32]

2.4 Finite element modeling

2.4.1 Model development. Mathematical model was developed to simulate the drying of a single pomace cube under MVD. The model set up and mesh grid is shown in Fig. 1.

2.4.1.1 Governing equations. The heat and moisture transfer during the MVD process was simulated using a nonequilibrium multiphase transport modeling approach that accounts for the *in situ* moisture vaporization within the porous solid matrix.[33] Eqn (6) was used as the governing equation for the transport of liquid moisture during the grape pomace cubes' drying. The transport of water vapor was modeled using:

$$\frac{\partial C_v}{\partial t} = D_v\left(\frac{\partial^2 C_v}{\partial x^2} + \frac{\partial^2 C_v}{\partial y^2}\right) + i \quad (11)$$

where, C_v is the concentration of water vapor (kg m^{-3}); D_v is the vapor diffusivity (m^2 s^{-1}); the term i is the internal moisture evaporation rate (kg m^{-3} s^{-1}).

Eqn (12) was used to model the heat transfer during the drying process in 2-D cartesian coordinate system.

$$\rho C_p \frac{\partial T}{\partial t} = k\left(\frac{\partial^2 T}{\partial x^2} + \frac{\partial^2 T}{\partial y^2}\right) + Q_{MW} - i\lambda \quad (12)$$

where, ρ is the material density (kg m^{-3}); C_p is the specific heat of the material (J^{-1} kg^{-1} K^{-1}); k is the thermal conductivity (W^{-1} m^{-1} K^{-1}); Q_{MW} is the heat absorption by the sample due to the MW heating (W); λ is the latent heat of water vaporization (2.26 $\times$ 10^5 J kg^{-1}); $i\lambda$ corresponds to the latent heat of evaporation due to the internal moisture evaporation. The magnitude of i is calculated according to Kar and Chen:[34]

$$i = h_{m,in} \cdot A_{in}\,(C_{v,s} - C_v) \quad (13)$$

where, A_{in} is the internal surface area per unit volume available for local evaporation (m^2 m^{-3}) and $h_{m,in}$ is the internal surface mass transfer coefficient (m s^{-1}), which were determined according to Kar and Chen;[34] $C_{v,s}$ is the water vapor concentration at the internal-surface of the porous solid matrix (kg m^{-3}). The reaction engineering approach (REA)[35] was implemented to determine the internal-surface water vapor concentration, with the detailed equations shown in Appendices A.

Although MW heating is always considered as a volumetric heating technology, its penetration into foods is limited, which depends on both the food properties as well as the MW wavelength. In general, the penetration depth of commercial MW radiation into solid foods range from 0.8 to 3.8 cm.[36,37] Considering the small dimension of the pomace cubes in this study, it is assumed that the initial MW power absorption was uniformly distributed in the samples. The heat absorption by MW heating can be estimated based on both a fully coupled electromagnetism model[38,39] or an empirical model.[40,41] In this study, the heat generation within the sample due to MW heating was estimated following a method introduced by Rakesh and Datta[42] and Salvador.[43] Specifically, Q_{MW} was expressed as a function of sample moisture loss (eqn (14)). The initial MW power absorption by the sample was estimated based on the temperature profile of the sample.

$$Q_{MW} = 2 \times 10^6\left(\frac{M_{DB_0}}{M_{DB}}\right)^{-4} \quad (14)$$

where, M_{DB_0} is the initial moisture content (kg water/kg dry mass) of the sample.

2.4.1.2 Initial conditions (IC) and boundary conditions (BC)

$$T = T_0,\ C_w = C_{w0},\ C_v = C_{v0} \text{ at } t = 0 \quad (15)$$

Side and bottom surfaces of cubes were set as zero-flux boundary to moisture transfer. The moisture removal from the pomace cubes only happened at the top exposed surface ($y = l$), with equivalent convective boundary conditions for heat and mass transfer set as:

$$-D_{eff}\frac{\partial M_{DB}}{\partial y} = h_m \varepsilon_w\left(\frac{C_{v,s}}{\varepsilon} - C_{v,b}\right) \quad \text{at } t > 0 \quad (16)$$

$$-D_v\frac{\partial C_v}{\partial y} = h_m \varepsilon_v\left(\frac{C_{v,s}}{\varepsilon} - C_{v,b}\right) \quad \text{at } t > 0 \quad (17)$$

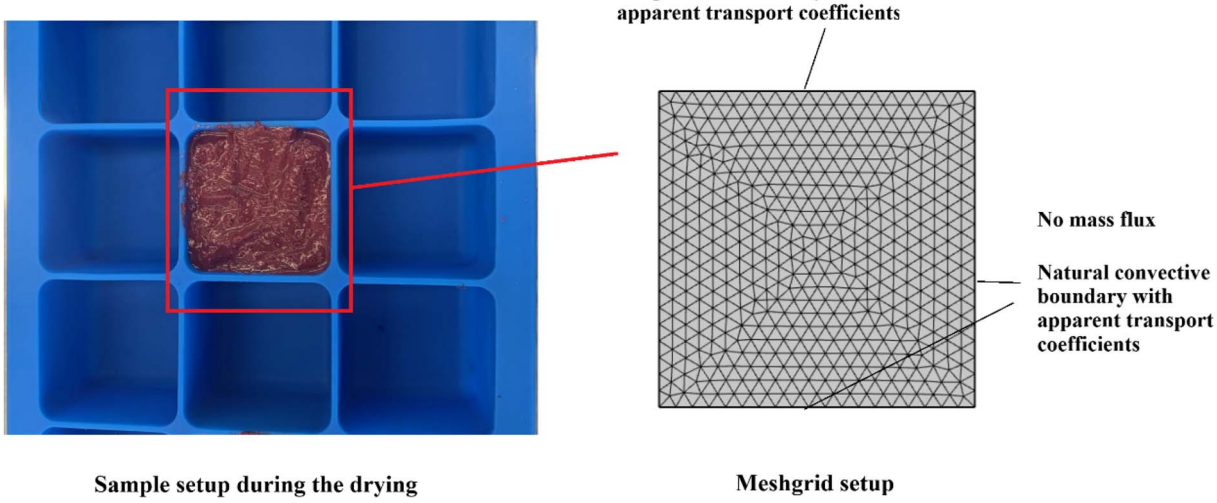

Fig. 1 Sample setup during the drying process and modeling system setup with mesh grid.

Table 1 Summary of model parameters

Parameter	Material	Value	Unit	Source
Length (initial)	Pomace	30.0	mm	Determined in this study
Initial moisture	Pomace	790	kg m^{-3}	
Initial temperature	Pomace	4.0	°C	
Effective moisture diffusivity	Pomace	D_{eff}	m^2 s^{-1}	
Specific heat	Pomace	1652–3325	J (kg^{-1} K^{-1})	44
Thermal conductivity	Pomace	0.125–0.420	W (m^{-1} K^{-1})	44
Density	Pomace	886–1128	kg m^{-3}	45 and 46
Porosity	Cookie	0.55–0.88		46
Enthalpy of water evaporation	Water	1857.4–2423.6	kJ kg^{-1}	8
Heat transfer coefficient	Air	18.5–22.6	W (m^{-2} K^{-1})	Determined in this study
Effective evaporative moisture transfer coefficient	Air	0.0435–0.0505	m s^{-1}	

$$-k\frac{\partial T}{\partial y} = h(T_s - T_a) - \lambda h_m \varepsilon_w \left(\frac{C_{v,s}}{\varepsilon} - C_{v,b}\right) \quad \text{at } t > 0 \qquad (18)$$

where, h_m was the effective evaporative moisture transfer coefficient (m s^{-1}); h was the convective heat transfer coefficient (W m^{-2} K^{-1}); C_w is the liquid moisture concentration (kg m^{-3}); $C_{v,b}$ is the water vapor concentration in the chamber environment (kg m^{-3}), which is assumed to be zero under highly vacuumed conditions; T_s and T_a were the temperature at material surface and the ambient (K); ε is the sample porosity; ε_w and ε_v are the saturation fractions of the surface area of pomace cubes covered by liquid and vapor moisture, respectively (Appendices A). The heat and moisture transfer coefficient were estimated following the methods introduced in;[28] The input parameters of the model are summarized in Table 1.

2.4.1.3 Model solving. The mathematical model was solved using COMSOL Multiphysics software (Version 5.6, Sweden) using a finite element method (FEM) which applied the Galerkin's method. An Intel® Core™ i7-13700 T processor (1.40 GHz) was used to run the software. The relative convergence tolerance of the iterative algorithms was set as 0.005. In total, 928 free triangular elements and 76 boundary elements were used to build the mesh grid. The maximum element size was 1.59×10^{-3} m and the minimum element size was 9.00×10^{-6} m.

2.4.2 Model validation. An additional set of experimental data, not used for model development, was obtained at 540, 1080, and 2160 W power and 8 kPa vacuum was used for model validation. The drying experiments were performed in triplicate. The average MC of the pomace cubes was measured using the methods introduced in previous sections. The prediction capability of both the Page model and the mechanistic model was determined quantitatively by plotting the experimental data against prediction values and calculating the adjusted coefficient of determination (R_{adj}^2) and root mean square error (RMSE).

$$R_{adj}^2 = 1 - \frac{\left(\frac{\sum_1^n \left(y_{exp,i} - y_{pre,i}\right)^2}{\sum_1^n \left(\overline{y_{exp,i}} - y_{pre,i}\right)^2}\right)(N-1)}{N-p-1} \qquad (19)$$

where, p is the number of predictors; N is the total sample size.

$$\mathrm{RMSE} = \sqrt{\frac{\sum_1^n \left(y_{exp,i} - y_{pre,i}\right)^2}{N}} \qquad (20)$$

where, $y_{exp,i}$ and $y_{pre,i}$ are experimental and predicted values of the studied variables, respectively; $\overline{y_{exp}}$ is the average experimental values of the studied variables.

2.5 Statistical analysis

All drying experiments were performed in triplicate, and the data were presented as mean ± standard deviation. All physicochemical measurements were taken in at least duplicate measurements at each drying time point, leading to at least six repetitions. The correlations between the variables were tested using a Pearson Correlation Matrix, with the statistical significance of each pair of the correlations evaluated using a *t*-test for exploratory analysis at a confidence level of 95% in the SPSS (IBM, Armonk, New York) software.

3 Results and discussion

3.1 Drying kinetics

The drying curves (moisture content and average drying rates of the sample against drying time) are shown in Fig. 2. For the MVD process, the drying showed two stages: (1) a short preheating followed by constant-rate drying stage of ~5 min, where the drying curve has a convex-straight shape, during which the free moisture was removed. The higher the input MW power, the shorter the first stage, suggesting higher heating efficiency at higher MW levels. (2) a falling-rate stage, where the drying curve has a concave shape, when the bound moisture was removed. Since the falling-rate stage dominates the drying process, it is suggested that the drying rate was controlled by internal moisture diffusion. This ensured the validity of determining the moisture diffusivity and modeling the drying process using the Fickian model. The highest drying rate achieved in the MVD process ranged from 0.0021 to 0.0064 kg water/kg dry mass/min, which increased with the increase in MW power. In comparison, the highest drying rate during the HA drying at 60 °C was 0.00036 kg water/kg dry mass/min, which was about 1/20 to 1/5 than that of the MVD. Specific energy consumption (SEC) of the drying process was also

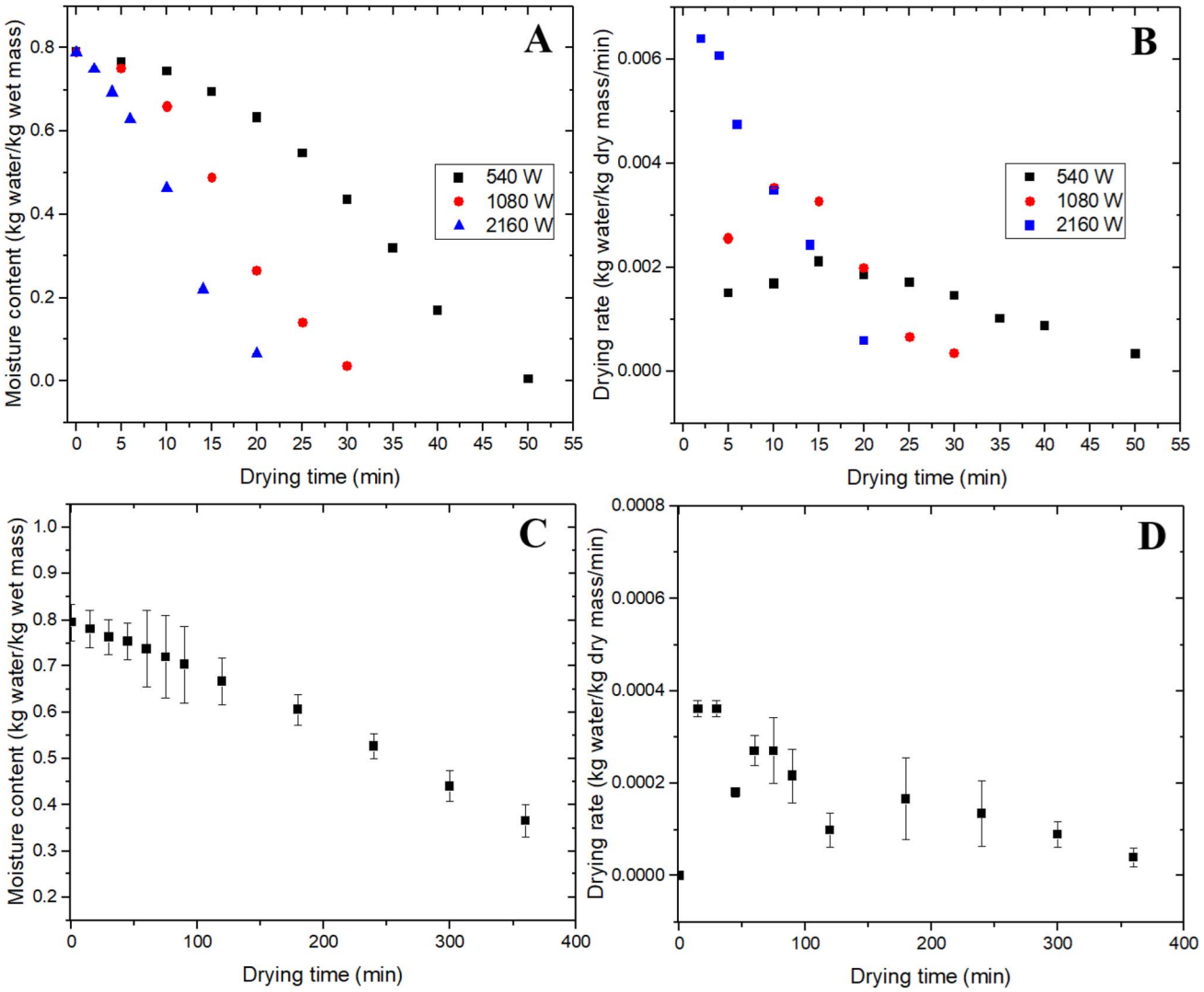

Fig. 2 (A) Drying curves and (B) drying rate curves of grape pomaces during the MVD process at 540, 1080, and 2160 W nominal MW power; and (C) drying curves and (D) drying rate curves of grape pomaces under the HA drying process at 60 °C.

evaluated and computed based on the total energy input and the amount of water removed from the pomace. The MVD required 5.7, 6.8, and 9.1 kJ g^{-1} water evaporated SEC at power levels 540, 1080, and 2160 W respectively in this study (standard deviation omitted due to low standard deviation in weight after triplicate drying). Drying at higher wattage provided a faster time to drying but required more energy; however, efficiency will likely increase with higher loading weights and larger scale equipment. The SEC of the MVD process was considerably lower than the energy consumption of grape pomace by forced convective drying (40.7 to 42.8 kJ g^{-1} water evaporated) and infrared film drying (14.6 to 21.2 kJ g^{-1} water evaporated).[47] This result suggests that MVD is an energy saving technology for drying grape pomace with enhanced sustainability.

3.1.1 Effective moisture diffusivity. The effective moisture diffusivity of the grape pomace during the drying process was determined piecewise using eqn (8) by taking the natural log of the original MR data. The correlation between the D_{eff} and the sample moisture at different MW power levels are shown in Fig. 3, which ranged from 4.5×10^{-8} to 4.2×10^{-7} m^2 s^{-1}. The effective moisture diffusivity showed an inverse correlation with moisture content, as the drying proceeded the moisture diffusivity increased. The results obtained in this study are in line with previous studies on MW drying of foods.[24,48] This observed trend could be attributed to the combined influence of multiple factors: (1) Temperature: D_{eff} values usually increase with the increase in sample temperature due to the activation of water molecules at higher temperatures;[49] (2) Moisture: D_{eff} values usually decrease with the decrease in sample moisture due to larger resistance to internal moisture diffusion at later drying stages;[50] (3) MW power: In general, higher MW power leads to higher D_{eff} values,[51] as indicated by the D_{avg} values in Table 2. In this study, since the input power of the magnetrons was kept constant throughout the drying, and the sample weight decreased during the drying, the power density (W g^{-1}) received by the sample increased with the drying time. This resulted in

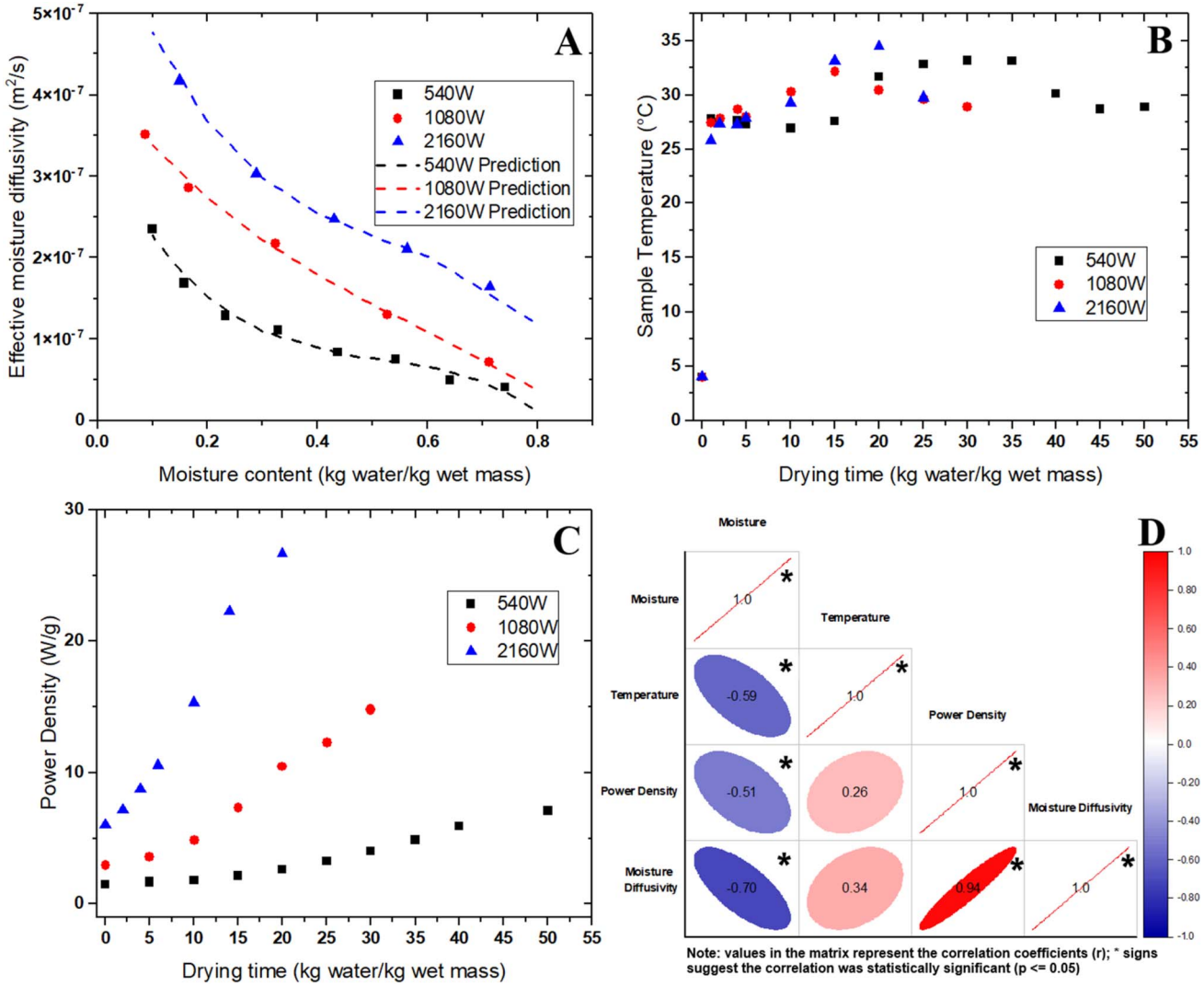

Fig. 3 (A) Effective moisture diffusivity in the grape pomace samples *versus* sample moisture; (B) sample surface temperature *versus* drying time; (C) specific power density of sample *versus* drying time; (D) pearson correlation matrix showing the correlation among sample temperature, moisture, power density and moisture diffusivity with pairwise statistical analysis.

higher, more efficient moisture diffusion at later drying stages; (4) Dielectric properties: the dielectric constant and loss factor decreased with the decrease in sample moisture, since the dried pomace had lower capability to store electrical energy and dissipate it as heat,[36] which led to less efficient absorption of the MW energy in the samples. The uncertainty values of the D_{eff} depended on the nominal values of it at each time points and ranged from 2.35% to 6.76% in this study.

Table 2 Regression coefficients of the polynomial model correlating the effective moisture diffusivity and sample moisture

Power level	540 W	1080 W	2160 W
Regression coefficients			
A	-1.6×10^{-6}	-5.4×10^{-7}	-1.9×10^{-6}
B	2.5×10^{-6}	9.5×10^{-7}	-3.1×10^{-6}
C	-1.4×10^{-6}	-8.9×10^{-7}	-1.9×10^{-6}
D	3.4×10^{-7}	4.2×10^{-7}	6.3×10^{-7}
D_{avg} ($m^2\ s^{-1}$)	1.1×10^{-7}	2.3×10^{-7}	3.4×10^{-7}
R^2_{adj}	0.992	0.998	0.993

To understand the main contributors of moisture diffusivity change, the change in temperature, moisture, and power density in the pomace during MVD were evaluated using a Pearson correlation matrix as shown in Fig. 3. The correlation coefficients suggested that sample moisture was statistically significantly (unadjusted) negatively correlated with the moisture diffusivity (−0.70 correlation coefficient), and the power density had a statistically significantly (unadjusted) positive correlation with the diffusivity (0.94 correlation coefficient). On the other hand, no statistically significant correlations were observed between the sample temperature, D_{eff} and power density. The results suggest that the powder density increase during the drying process probably contributed the most to the increase in D_{eff} values. Further analysis on the dielectric properties, as well as moisture and temperature distribution

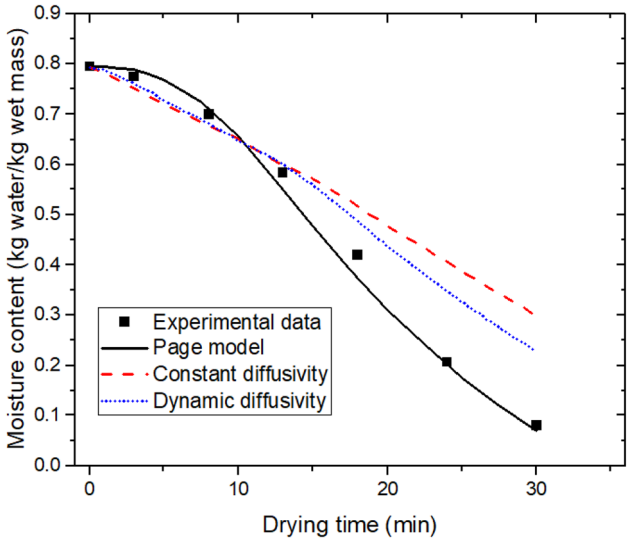

Fig. 4 Model validation by comparing the simulation results from different models with the experimental data at 1080 W nominal MW power.

measurements, will be required to provide a better mechanistic understanding of this phenomena.

To validate the mathematical models developed in Section 3.1.2, the effective moisture diffusivity was incorporated into the moisture transfer governing equation in the mechanistic model described in Section 2.4. Three modeling scenarios were compared: (1) Page model; (2) Mechanistic model with a constant effective moisture diffusivity value (D_{avg}); (3) Dynamic moisture diffusivity model (D_{eff}). The simulation results of sample moisture during the drying process under 1080 W nominal MW power as an example and compared with the modeling results are presented in Fig. 4. The Page model fitted the experimental data well (R_{adj}^2 ranged from 0.992 to 0.998, as shown in Table 3). However, it should be noted that empirical modeling results cannot be used for extrapolation. The modeling results with the constant diffusivity value showed deviations from the experimental data (R_{adj}^2 ranged from 0.970 to 0.978), particularly, under-estimation of sample moisture was observed at high-moisture ranges, and over-estimation was observed at low-moisture ranges. This was because the D_{eff} increased with the decrease in sample moisture. In comparison, the dynamic moisture diffusivity model showed better predictability than modeling results with constant diffusivity values (R_{adj}^2 ranged from 0.979 to 0.985). Although the R_{adj}^2 was not as high as the Page model, a mechanistic model could be used for prediction in a broader range of conditions, which would be more helpful for optimizing the drying conditions. The lack of fit of modeling results could be attributed to several reasons: (1) the assumptions on no shape changes of samples during the drying; (2) lack of a fully coupled electromagnetic field simulation to accurately account for the MW effect on heat transfer.

3.2 Color change

The grape color is mainly attributed to anthocyanins, which are oxygen and heat labile. The color metrics (L^*, a^*, b^*) of the grape pomace during the drying process were plotted against the moisture content of the pomace (Fig. 5 A and B). During the MVD process. The L^* values ranged from 32.35 to 42.82, a^* values ranged from 9.33 to 11.84, b^* values ranged from 12.03 to 17.28, respectively. The influence of the MW power and drying time on the color change was not significant, indicating the MVD process maintained the product color well. Under HA drying, the L^* values reduced significantly from 40.82 to 21.03 at the end of the drying. The a^* and b^* ranged from 10.31 to 15.19, and 15.43 to 18.98, respectively, with no apparent trends. The results suggested that MVD could better preserve the natural color in the grape pomace compared to applying HA, which should be due to the relatively moderate drying temperature and low oxygen exposure during the drying process. This enhanced color preservation renders a distinctive opportunity to valorize the dried pomace into future food ingredients, such as a natural colorant.

Table 3 Summary of model validation results

	540 W	1080 W	2160 W
Page model			
k	5.07×10^{-5}	5.70×10^{-4}	5.59×10^{-3}
n	2.793	2.526	2.065
Adjusted R^2	0.998	0.992	0.994
RMSE	0.038	0.080	0.065
Mechanistic-D_{avg}			
Adjusted R^2	0.978	0.973	0.970
RMSE	0.135	0.146	0.151
Mechanistic-dynamic D_{eff}			
Adjusted R^2	0.983	0.985	0.979
RMSE	0.112	0.105	0.130

3.3 Total polyphenolic content

The change in TPC in the grape pomace during the drying process under different input MW power levels is displayed in Fig. 5C against the moisture content. The values were adjusted to the same water content as the original pomace to be able to compare the TPC on the same basis. The TPC increased from 1.05 to 2.58 mg GAE/g dry pomace after the drying (corresponding up to a 142.3% increase). The results suggested that the MW power level had no significant influence ($p > 0.05$) on the TPC in the dried grape pomace. Therefore, a generic second order polynomial equation was used to correlate the TPC change with sample moisture change during the MVD process to study the phenolics change kinetics using a nonlinear regression approach (Fig. 5C). The R_{adj}^2 was 0.942 and the RMSE was 0.417, which suggested good fit. Such phenomena have been reported in the MW drying of other plant materials[52] and should be attributed to a coupled effect of various contributing factors. The anthocyanins in grape skins are heat sensitive and usually degrade following a first-order reaction kinetics, of which the degradation rate increases with temperature.[53,54] In addition, MW heating may lead to electroporation

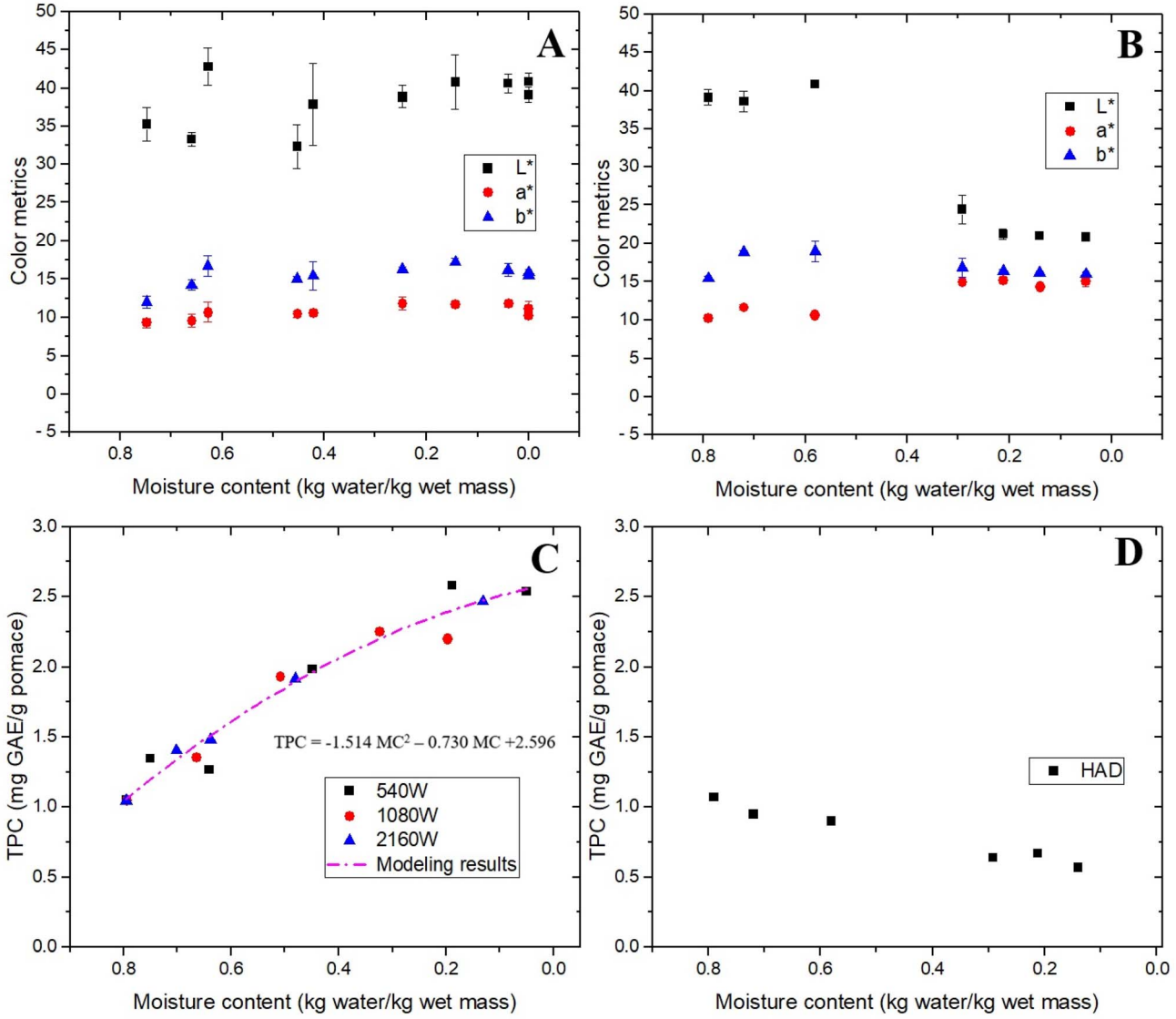

Fig. 5 Changes in color metrics (L^*, a^*, b^*) during (A) MVD and (B) HA drying; and changes in Total Polyphenolic Content (TPC) during (C) MVD and (D) HA drying processes in the grape pomace against sample moisture, and regression modeling results of TPC.

effect in the plant cells, which increases the extraction yield of phenolic compounds from grape skin. Mechanistically, when plant cells are subjected to the MW, polar molecules such as water, form dipoles under the frequency oscillating electromagnetic field and physically move within the cell, causing physical damage (such as micro-holes) in the cell wall. These holes in the cell wall can cause the releasing of cytoplasm and vacuole content, leading to freeing up of anthocyanins and other polyphenols for easier extraction. Similar effects have also been achieved in other electromagnetic-wave processing of food. For example, Athanasiadis *et al.*[55] found that TPC in grapes was increased after pulsed electric field processing. Romero-Díez *et al.*[56] found MW-assisted extraction doubled anthocyanin yield compared to solvent extraction alone from wine lees. In comparison, the TPC in the HA-dried pomace was 0.57 mg GAE/g dry pomace, which corresponds to 46.7% reduction. During MVD, the water boiling temperature and oxygen concentration were significantly decreased compared to under atmospheric conditions, which likely significantly reduced the rate of polyphenol degradation compared to HA drying. The findings suggest that MVD holds strong promise in upcycling the grape pomace as a valuable resource for extracting the bioactive polyphenolic compounds such as the natural red colorants or nutraceuticals. Additionally, successful valorization of this bioresource will reduce the negative environmental impacts associated with its disposal, and improve the sustainability of the grape production and processing systems.

Conclusion

This study contributed valuable insights into the moisture transfer mechanisms and quality change kinetics during microwave vacuum drying process of juicing grape pomace. The effective moisture diffusivity ranged from 4.5×10^{-8} to $4.2 \times$

10^{-7} m^2 s^{-1}, which was correlated with sample moisture and microwave power using regression models and validated with experimental data using a nonequilibrium multiphase mechanistic modeling approach. Color of the pomace did not change significantly during the drying, while the total polyphenolic content increased by up to 142.3%, leading to a higher quality upcycled product. The phenolic content change was modeled using a 2nd order polynomial equation with the sample moisture. The quantitative data and mathematical models set basis for estimating and optimizing the pomace drying process effectively for better nutrient preservation and value-added utilization of this food processing byproduct. Meanwhile, the investigation methods developed in this study have the potential to be applied for studying the moisture transfer characteristics during microwave vacuum drying of other foods and agricultural products.

Author contributions

Conceptualization, O. I. P.-Z. and C. C.; methodology, V. S. and C. C.; investigation, V. S.; formal analysis V. S. and C. C.; writing—original draft preparation, V. S.; writing—review and editing, V. S., O. I. P.-Z. and C. C.; supervision, C. C. All authors have read and agreed to the published version of the manuscript.

Conflicts of interest

The authors declare no conflict of interest.

Data availability

All the data generated or analyzed during this study are included in the manuscript.

Appendix

The reaction engineering approach (REA) approach[35] is implemented to determine the internal-surface water vapor concentration:

$$C_{v,s} = \exp\left(\frac{-\Delta E_v}{RT}\right) C_{v,sat} \quad (A.1)$$

where, $C_{v,sat}$ is the saturated vapor concentration at temperature T (kg m^{-3}), of which the formula was written in eqn (A.2); ΔE_v is the relative activation energy (J mol^{-1}), which is a 'fingerprint' parameters of food material determined from the moisture curve experimentally eqn (A.3).

$$C_{v,sat} = 4.844 \times 10^{-9} (T - 273.15)^4 - 1.4807 \times 10^{-7}(T - 273.15)^3 + 2.6572 \times 10^{-5}(T - 273.15)^2 - 4.8613 \times 10^{-5}(T - 273.15) + 8.342 \times 10^{-3} \quad (A.2)$$

$$\Delta E_v = -RT_s \ln\left[\frac{-\frac{dM_{DB}}{dt}\frac{1}{h_m A} + \rho_{v,b}}{C_{v,sat}(T_s)}\right] \quad (A.3)$$

where, dM_{DB}/dt is the rate of moisture removal that was determined in the experiments (kg m^{-3} s^{-1}); A is the surface area of the cookie (m^2); the relative activation energy of the drying was expressed as a function of average sample moisture.

$$\frac{\Delta E_v}{\Delta E_{v,b}} = f\left(\overline{MC} - MC_b\right) \quad (A.4)$$

where, $\overline{MC}$ and MC_b are the average moisture content and the lowest equilibrium moisture content determined from experiments (kg moisture/kg dry mass).

Saturation fractions of surface area covered by liquid water and water vapor were determined as:

$$\rho_w \varepsilon_w = \frac{m_w}{V} = C_w \quad (A.5)$$

$$\varepsilon_v = \varepsilon - \varepsilon_w \quad (A.6)$$

where, ρ_w is the density of water (kg m^{-3}); m_w is the mass of water in the sample; V is the volume of the sample (m^3).

The effective vapor diffusivity is determined as:[57]

$$D_v = D_{v0} \times \frac{\varepsilon}{\tau} \quad (A.7)$$

where, D_{v0} is the water vapor diffusivity (m^2 s^{-1}), which depends on the vapor temperature; τ is the tortuosity of the pomace matrix.

For food and biological materials, D_{v0} could be expressed as:

$$D_{v0} = 2.09 \times 10^{-5} + 2.137 \times 10^{-7} (T - 273.15) \quad (A.8)$$

The tortuosity (τ) in the food materials generally correlated with the porosity, which could be expressed as:

$$\tau = \varepsilon^{-n} \quad (A.9)$$

where, n is a value between 0 and 0.5, and a value of 0.5 is used in this study according to Putranto and Chen.[58]

$$D_{AB} = 2.3056 \times 10^{-5} [9.81 \times 10^4/(T_a - 273)] \times (T_a/273)^{1.81} \quad (A.10)$$

where, T_a is the air temperature (K).

Acknowledgements

The authors thank the Seneca Foods Foundation Pilot Plant at Cornell AgriTech for technical assistance in pilot processing. This research was funded by the U.S. Department of Agriculture National Institute of Food and Agriculture, Federal Capacity Funds Multistate Project NC10203, New York State Department of Agriculture & Markets, Concord Grape Research, and New York Wine and Grape Foundation.

References

1 USDA-NASS. U.S. Department of Agriculture, National Agricultural Statistics Service, Noncitrus Fruits and Nuts 2019 Summary. *Noncitrus Fruits Nuts 2019 Summ.* 2020, vol.

12, p. 42. https://downloads.usda.library.cornell.edu/usda-esmis/files/zs25x846c/0g3551329/qj72pt50f/ncit0520.pdf.
2 M. P. Zacharof, Grape Winery Waste as Feedstock for Bioconversions: Applying the Biorefinery Concept, *Waste Biomass Valorization*, 2017, **8**, 1011–1025.
3 M. Spinei and M. Oroian, The Potential of Grape Pomace Varieties as a Dietary Source of Pectic Substances, *Foods*, 2021, **10**(4), 867.
4 L. F. Ribeiro, R. H. Ribani, T. M. G. Francisco, A. A. Soares, R. Pontarolo and C. W. I. Haminiuk, Profile of bioactive compounds from grape pomace (Vitis vinifera and Vitis labrusca) by spectrophotometric, chromatographic and spectral analyses, *J. Chromatogr. B:Anal. Technol. Biomed. Life Sci.*, 2015, **1007**, 72–80, DOI: 10.1016/j.jchromb.2015.11.005.
5 N. Agarwal, V. Shukla, N. Kolba, C. Jackson, J. Cheng, O. I. Padilla-zakour, *et al.*, Comparing the Effects of Concord Grape (Vitis labrusca L.) Puree, Juice, and Pomace on Intestinal Morphology, Functionality, and Bacterial Populations *In Vivo* (Gallus gallus), *Nutrients*, 2022, **14**, 3539.
6 J. H. El Achkar, T. Lendormi, Z. Hobaika, D. Salameh, N. Louka, R. G. Maroun, *et al.*, Anaerobic digestion of nine varieties of grape pomace: Correlation between biochemical composition and methane production, *Biomass Bioenergy*, 2017, **107**, 335–344, DOI: 10.1016/j.biombioe.2017.10.030.
7 M. Migliori, D. Gabriele, B. De Cindio and C. M. Pollini, Modelling of high quality pasta drying: Quality indices and industrial application, *J. Food Eng.*, 2005, **71**, 242–251.
8 C. Chen, C. Venkitasamy, W. Zhang, L. Deng, X. Meng and Z. Pan, Effect of step-down temperature drying on energy consumption and product quality of walnuts, *J. Food Eng.*, 2020, **285**, 110105, DOI: 10.1016/j.jfoodeng.2020.110105.
9 W. P. Zhang, C. Chen, Z. Pan, H. W. Xiao, L. Xie, Z. J. Gao, *et al.*, Design and performance evaluation of a pilot-scale pulsed vacuum infrared drying (PVID) system for drying of berries, *Drying Technol.*, 2020, **38**, 1340–1355, DOI: 10.1080/07373937.2019.1639725.
10 C. Chen. *Characteristics and Mechanisms of Walnut Drying under Hot Air and Infrared Heating*. UNIVERSITY OF CALIFORNIA; 2020.
11 T. Sokač, V. Gunjević, A. Pušek, A. J. Tušek, F. Dujmić, M. Brnčić, *et al.*, Comparison of Drying Methods and Their Effect on the Stability of Graševina Grape Pomace Biologically Active Compounds, *Foods*, 2022, **11**(1), 112.
12 A. M. Goula, K. Thymiatis and K. Kaderides, Valorization of grape pomace: Drying behavior and ultrasound extraction of phenolics, *Food Bioprod. Process.*, 2016, **100**, 132–144, DOI: 10.1016/j.fbp.2016.06.016.
13 A. Tseng and Y. Zhao, Effect of Different Drying Methods and Storage Time on the Retention of Bioactive Compounds and Antibacterial Activity of Wine Grape Pomace (Pinot Noir and Merlot), *J. Food Sci.*, 2012, **77**(9), H192–H201.
14 Y. Sui, J. Yang, Q. Ye, H. Li and H. Wang, Infrared, Convective, and Sequential Infrared and Convective Drying of Wine Grape Pomace, *Drying Technol.*, 2014, **32**, 686–694.
15 J. C. Hogervorst, U. Miljić and V. Puškaš. Extraction of Bioactive Compounds from Grape Processing By-Products. *Handbook of Grape Processing By-Products: Sustainable Solutions*. 2017. pp. 105–135.
16 M. Leiker and M. A. Adamska, Energy efficiency and drying rates during vacuum microwave drying of wood, *Holz Roh-Werkst.*, 2004, **62**, 203–208.
17 D. J. Griffiths. *Introduction to Electrodynamics*. Prentice Hall; 1999.
18 P. S. Sunjka, T. J. Rennie, C. Beaudry and G. S. V. Raghavan, Microwave-convective and microwave-vacuum drying of cranberries: A comparative study, *Drying Technol.*, 2004, **22**, 1217–1231.
19 Z. W. Cui, L. J. Sun, W. Chen and D. W. Sun, Preparation of dry honey by microwave-vacuum drying, *J. Food Eng.*, 2008, **84**, 582–590.
20 J. Dumpler and C. I. Moraru, Modeling the drying kinetics of microwave vacuum drying of concentrated skim milk: correlation of dielectric properties, drying stages, and specific energy demand at pilot scale, *Drying Technol.*, 2023, **41**, 17–33, DOI: 10.1080/07373937.2022.2080220.
21 C. Chen and Z. Pan, An overview of progress, challenges, needs and trends in mathematical modeling approaches in food drying, *Drying Technol.*, 2023, **41**, 2586–2605.
22 M. Dak and N. K. Pareek, Effective moisture diffusivity of pomegranate arils under going microwave-vacuum drying, *J. Food Eng.*, 2014, **122**, 117–121, DOI: 10.1016/j.jfoodeng.2013.08.040.
23 J. S. Roberts, D. R. Kidd and O. Padilla-Zakour, Drying kinetics of grape seeds, *J. Food Eng.*, 2008, **89**, 460–465.
24 G. Dadali, D. K. Apar and B. Özbek, Estimation of effective moisture diffusivity of okra for microwave drying, *Drying Technol.*, 2007, **25**, 1445–1450.
25 A. Figiel and A. Michalska, Overall quality of fruits and vegetables products affected by the drying processes with the assistance of vacuum-microwaves, *Int. J. Mol. Sci.*, 2017, **8**(1), 71.
26 A. L. Waterhouse. Polphenolics. in: *Handbook of Food Analytical Chemistry*. 2005.
27 A. O. A. C., *Anal. Methods*, 1999, 124–130.
28 C. Chen, C. Venkitasamy, W. Zhang, R. Khir, S. Upadhyaya and Z. Pan, Effective moisture diffusivity and drying simulation of walnuts under hot air, *Int. J. Heat Mass Transfer*, 2020, **150**, 119283.
29 J. Crank. *The Mathematics of Diffusion*. 2nd edn Oxford University Press; 1975.
30 B. Singh and A. K. Gupta, Mass transfer kinetics and determination of effective diffusivity during convective dehydration of pre-osmosed carrot cubes, *J. Food Eng.*, 2007, **79**, 459–470.
31 J. Shi, Z. Pan, T. H. McHugh, D. Wood, E. Hirschberg and D. Olson, Drying and quality characteristics of fresh and sugar-infused blueberries dried with infrared radiation heating, *Lwt*, 2008, **41**, 1962–1972.
32 J. P. Holman. *Experimental Methods for Engineers*. 2012.
33 C. Chen, S. Upadhyaya, R. Khir and Z. Pan, Simulation of walnut drying under hot air heating using

a nonequilibrium multiphase transfer model, *Drying Technol.*, 2020, **40**, 987–1001.
34 S. Kar and X. D. Chen, Modeling moisture transport across porcine skin using reaction engineering approach and examination of feasibility of the two-phase approach, *Chem. Eng. Commun.*, 2011, **198**, 847–885.
35 X. D. Chen and A. Putranto. *Reaction Engineering Approach I. Modeling Drying Processes*. 2013. pp. 34–120.
36 J. Tang, Unlocking Potentials of Microwaves for Food Safety and Quality, *J. Food Sci.*, 2015, **80**, E1776–E1793.
37 US Department of Agriculture. Cooking with Microwave Ovens. 2013**1–16**. **https://www.fsis.usda.gov/food-safety/safe-food-handling-and-preparation/food-safety-basics/cooking-microwave-ovens**.
38 H. Zhang and A. K. Datta, Microwave power absorption in single- and multiple-item foods, *Food Bioprod. Process.*, 2003, **81**, 257–265.
39 J. Chen, K. Pitchai, D. Jones and J. Subbiah, Effect of decoupling electromagnetics from heat transfer analysis on prediction accuracy and computation time in modeling microwave heating of frozen and fresh mashed potato, *J. Food Eng.*, 2014, **144**, 45–57, DOI: **10.1016/j.jfoodeng.2014.07.013**.
40 M. S. Ukidwe, A. K. Datta, C. Koh, S. Tibos and J. Bows, Coupled transport and poromechanics model to understand quality evolution during sequential drying, *Chem. Eng. Sci.*, 2023, **280**(2), 119010.
41 D. Wang, X. Li, X. Hao, J. Lv and X. Chen, The Effects of Moisture and Temperature on the Microwave Absorption Power of Poplar Wood, *Forests*, 2022, **13**(2), 309.
42 V. Rakesh and A. Datta, Microwave puffing: mathematical modeling and optimization, *Procedia Food Sci.*, 2011, **1**, 762–769, DOI: **10.1016/j.profoo.2011.09.115**.
43 A. Salvador. *Mathematical Modeling and Computational Simulation of Multiphase Transport and Structural Deformation in Porous Food during Microwave Vacuum Drying*. UNIVERSIDADE FEDERAL DE SANTA CATARINA CENTRO TECNOLÓGICO; 2023.
44 H. Samimi Akhijahani and J. Khodaei, Investigation of specific heat and thermal conductivity of rasa grape (Vitis vinifera L.) as a function of moisture content, *World Appl. Sci. J.*, 2013, **22**, 939–947.
45 N. Ageyeva, A. Tikhonova, B. Burtsev and E. Globa, Physicochemical parameters of grape pomace subject to grape processing technology applied, *E3S Web Conf.*, 2021, **285**, 05019.
46 C. Badouard, F. Bogard, C. Bliard, M. Lachi, B. Abbes and G. Polidori, Development and characterization of viticulture by-products for building applications, *Constr. Build. Mater.*, 2021, **302**, 0–16.
47 E. C. Dolgun, G. Karaca and M. Aktaş, Performance analysis of infrared film drying of grape pomace using energy and exergy methodology, *Int. Commun. Heat Mass Transfer*, 2020, **118**, 104827, DOI: **10.1016/j.icheatmasstransfer.2020.104827**.
48 G. P. Sharma and S. Prasad, Effective moisture diffusivity of garlic cloves undergoing microwave-convective drying, *J. Food Eng.*, 2004, **65**, 609–617.
49 W. Zhang, C. Chen, Z. Pan and Z. Zheng, Vacuum and infrared-assisted hot air impingement drying for improving the processing performance and quality of poria cocos (Schw.) wolf cubes, *Foods*, 2021, **10**(5), 992.
50 Z. Zheng, S. Wei, W. Xie, L. Ren, B. Fan, H. Fu, *et al.*, Determination and comparison of effective moisture diffusivity of carrot (core and cortex) during hot air drying, *J. Food Process Eng.*, 2022, 1–18.
51 T. Gulati, H. Zhu and A. K. Datta, Coupled electromagnetics, multiphase transport and large deformation model for microwave drying, *Chem. Eng. Sci.*, 2016, **156**, 206–228.
52 A. Snoussi, I. Essaidi, H. Ben Haj Koubaier, H. Zrelli, I. Alsafari, T. Živoslav, *et al.*, Drying methodology effect on the phenolic content, antioxidant activity of Myrtus communis L. leaves ethanol extracts and soybean oil oxidative stability, *BMC Chem*, 2021, **15**, 1–11, DOI: **10.1186/s13065-021-00753-2**.
53 D. Serea, N. N. Condurache, I. Aprodu, O. E. Constantin, G. E. Bahrim, N. Stănciuc, *et al.*, Thermal Stability and Inhibitory Action of Red Grape Skin Phytochemicals against Enzymes Associated with Metabolic Syndrome, *Antioxidants*, 2022, **11**(1), 118.
54 B. M. Muche, R. A. Speers and H. P. V. Rupasinghe, Storage Temperature Impacts on Anthocyanins Degradation, Color Changes and Haze Development in Juice of "Merlot", *"Ruby" Grapes (Vitis vinifera). Front Nutr*, 2018, **5**, 1–9.
55 V. Athanasiadis, T. Chatzimitakos, K. Kotsou, D. Kalompatsios, E. Bozinou and S. I. Lalas, Polyphenol Extraction from Food (by) Products by Pulsed Electric Field: A Review, *Int. J. Mol. Sci.*, 2023, **24**(21), 15914.
56 R. Romero-Díez, M. Matos, L. Rodrigues, M. R. Bronze, S. Rodríguez-Rojo, M. J. Cocero, *et al.*, Microwave and ultrasound pre-treatments to enhance anthocyanins extraction from different wine lees, *Food Chem.*, 2019, **272**, 258–266, DOI: **10.1016/j.foodchem.2018.08.016**.
57 C. Chen and Z. Pan, Heat and moisture transfer studies on walnuts during hot air drying in a fixed-bed column dryer, *Appl. Therm. Eng.*, 2021, **199**, 117554, DOI: **10.1016/j.applthermaleng.2021.117554**.
58 A. Putranto, X. D. Chen, Z. Xiao and P. A. Webley, Modeling of high-temperature treatment of wood using the reaction engineering approach (REA), *Bioresour. Technol.*, 2011, **102**, 6214–6220, DOI: **10.1016/j.biortech.2011.02.053**.